

Energy transfer, proton transfer and electron transfer reactions within zeolites

V. Ramamurthy,*^a P. Lakshminarasimhan,^a Clare P. Grey*^b and Linda J. Johnston*^c

^a Department of Chemistry, Tulane University, New Orleans, LA 70118, USA.

E-mail: murthy@mailhost.tcs.tulane.edu

^b Department of Chemistry, State University of New York, Stony Brook, NY 11794-3400, USA

^c Steacie Institute for Molecular Sciences, National Research Council of Canada, Ottawa, Ontario, Canada K1A 0R6

Received (in Cambridge, UK) 22nd May 1998, Accepted 26th June 1998

The chemistry of olefins in zeolites illustrates both the potential complexity and utility of zeolites as reaction media. Of particular interest are the changes in product selectivity that result from carrying out oxidation reactions in the constrained space of the zeolite cavity. Since zeolites are capable of promoting proton and electron transfer reactions one needs to be particularly careful in the choice of a zeolite as a reaction medium.

Introduction

Much of our understanding of the reactivity of organic molecules is based on experiments conducted either in the gas phase or in an isotropic liquid phase. Studies conducted in these media have provided empirical rules which help us to predict or rationalize the behavior of molecules in new environments. Although this has been successful in some cases, it is still difficult to predict the behavior of a molecule enclosed in, for example, a biological matrix or a solid assembly. In part, this is because many interactions between the reactant and the medium are often ignored, since it is not always straightforward to predict the effect of these interactions on chemical reactions. Recognizing the complexity of natural systems, and being inspired by them, chemists have utilized a number of organized media to study, and possibly alter, the behavior of included molecules. Examples of organized media which have been investigated include molecular crystals, inclusion complexes, liquid crystals, micelles and related assemblies such as vesicles,

microemulsions and membranes, monolayers, Langmuir–Blodgett films, surfaces (silica, clay and zeolites) and, more recently, natural systems such as proteins and DNA.¹ In this review we are concerned with one such organized/confined medium, namely a zeolite.²

In the past, most photochemistry in zeolites has been restricted to reactions of carbonyl systems.³ The extension of these studies to olefinic systems has demonstrated the complexity of zeolites as reaction media. The chemistry is complicated by both proton and electron transfer processes in which the zeolites themselves participate. This review summarizes a number of studies carried out in our laboratories that demonstrate this complexity of the chemistry. We aim however to show that much of the chemistry can be rationalized by careful characterization of the zeolites and the reaction intermediates by a variety of techniques including MAS NMR and time resolved laser spectroscopy. X and Y zeolites are used as the reaction media.

Structural features of zeolites

Zeolites are inorganic microporous and microcrystalline materials capable of complexing or adsorbing small and medium-sized organic molecules. $[\text{SiO}_4]^{4-}$ and $[\text{AlO}_4]^{5-}$ tetrahedra form the primary building blocks of zeolites.² These tetrahedra are linked by all their corners to form channels and cages or cavities with discrete sizes. The total framework charge of an aluminium-

V. Ramamurthy is the Bernard–Baus Professor of Chemistry at Tulane University in New Orleans. Previously, he was on the faculty at Indian Institute of Science, Bangalore, India (1978–1987) and on the staff of Central Research, DuPont, Wilmington (1987–1994). Following his undergraduate education in India his training in photochemistry was performed under the stewardships of R. S. H. Liu (Univ. Hawaii), P. de Mayo (Univ. Western Ontario) and N. J. Turro (Columbia Univ.) His research interests include the study of molecules in constrained media, solid state photochemistry and catalysis.

Pranatharthiharan Lakshminarasimhan (known as pH) came to USA in 1996 after completing his undergraduate education in India. He obtained a BSc in chemistry (1994) from the University of Madras and a MSc in Chemistry (1996) from the Indian Institute of Technology, Madras. Currently he is working towards a PhD degree at Tulane University and his project involves photochemical studies of organic molecules within zeolites.

Clair P. Grey obtained a BA in Chemistry from the University of Oxford in 1987. Her DPhil studies were carried out with Professors A. K. Cheetham and C. M. Dobson at Oxford. After receiving a DPhil (1991), she spent a year in the University of Nijmegen in Professor W. S. Veeman's Laboratory, as a Royal

Society Postdoctoral Fellow, followed by two years as a visiting scientist at DuPont CR&D, Wilmington, Delaware with Dr A. J. Vega. She joined the faculty at SUNY Stony Brook in 1994, as an Assistant Professor, and was promoted to an Associate Professor in 1997. She is the recipient of an NSF National Young Investigator Award (1994), a Cottrell Scholarship (1997), a Dupont Young Professor Award (1977), and Camille and Henry Dreyfus Teacher-Scholar Award (1998) and is currently Alfred P. Sloan Foundation Research Fellow. Her research interests include the use of solid state NMR and diffraction methods to study structure and gas adsorption on catalysts and zeolites, conductivity in ionic conductors, battery materials, and the development and application of new solid-state NMR methodology.

Linda J. Johnston obtained a PhD from the University of Western Ontario, London, Ontario in 1983 under the supervision of Professor P. de Mayo. Following postdoctoral work with Drs K. U. Ingold and J. C. Scaiano she joined the staff at the National Research Council Canada, Ottawa, in 1986. She is currently a senior research officer in the Chemical Biology Program of the Steacie Institute for Molecular Sciences. Research interests include kinetic and mechanistic studies of radical ion chemistry and photochemistry in organized media.

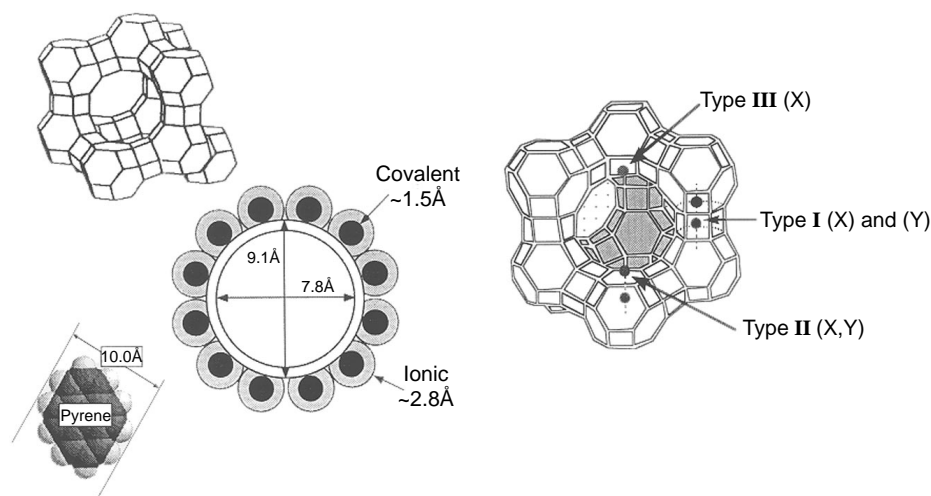
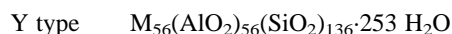
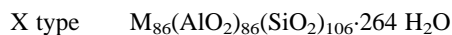


Fig. 1 The basic structural unit of X and Y zeolites. The entrance diameter of a supercage is shown on the left with the dimensions of a guest molecule, pyrene. The cation locations within a supercage are shown in colored circles.

containing zeolite is negative and hence must be balanced by an exchangeable cation, often an alkali or alkaline-earth metal cation. Zeolites can, thus, be represented by the empirical formula $M_{2/n} \cdot Al_2O_3 \cdot xSiO_2 \cdot yH_2O$, where M are the typically exchangeable cations of valence n (typically Na, Ca, Mg, *etc.*), x and y are integers. The two synthetic forms of faujasite are referred to as zeolite X and Y and have the following typical unit cell composition:

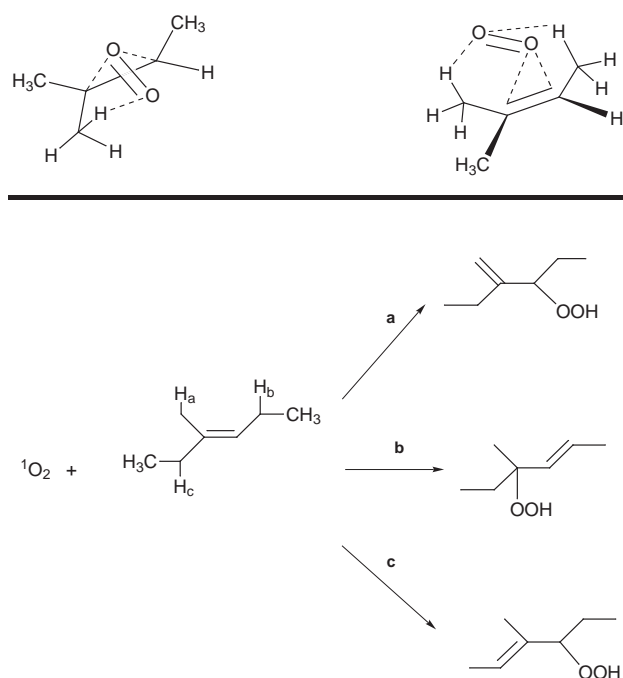


where M is a monovalent cation. The faujasite framework has two main cages. The large supercage results from an assembly of the basic units, the 'sodalite cages'. While sodalite cages are too small to accommodate organic molecules, the spherical supercages are approximately 13 Å in diameter. Access to the supercages is afforded by four 12-membered ring windows about 9 Å in diameter, which are tetrahedrally distributed about the center of the supercages. The supercages thus form a three-dimensional network with each supercage connected to four other supercages through the 12-ring window. The unit cell of X and Y zeolite consists of eight supercages.

The charge-compensating cations are known to occupy at least three different positions in zeolites X and Y.⁴ As illustrated in Fig. 1, the first type (site I), with *ca.* 4–8 cations per unit cell, is located in the hexagonal prism faces between the sodalite units. The second type (site II), with 32 ions per unit cell (in both X and Y), is located in the open hexagonal faces. The third type (site III) is only substantially occupied in X zeolite (and CsY) and is located on the walls of the larger cavity. Other sites (II' and I') exist in the sodalite cage, but only cations at sites II and III are expected to be readily accessible to the organic molecule adsorbed within a supercage. Note that in certain circumstances substantial rearrangements of these cations can occur, involving migrations of cations between the cages.⁵

Selectivity during singlet oxygen mediated oxidation of alkenes

Singlet oxygen is known to react with electron-rich alkenes *via* a 2 + 2 addition process.⁶ When the alkene contains allylic hydrogen atoms, however, the 'ene reaction' is the dominant pathway.⁷ Alkenes with more than one distinct allylic hydrogen yield several hydroperoxides (Scheme 1). With a medium such as a zeolite, we envisioned that it should be possible to achieve high selectivity during the singlet oxygen ene reaction. The results of this study are presented below, as an example to



Scheme 1

illustrate the uniqueness, complexities and challenges of zeolites as reaction media.

The generation of singlet oxygen for the subsequent oxidation of alkenes requires assembling three species—oxygen, alkene and a sensitizer—within the internal structure of a zeolite. Monomeric thionin is a useful sensitizer for the generation of singlet oxygen; thionin is easily exchanged into NaY zeolite by stirring the dye with hydrated NaY in water. While the dye, as exchanged, remains in the dimeric form within hydrated NaY, careful dehydration of the zeolite results in a color change.⁸ The hydrated dye is violet and upon drying the dye becomes blue. Upon thorough drying, thionin adopts a monomeric structure (Fig. 2) and excitation of a blue zeolite containing monomeric thionin shows an emission from singlet oxygen. Singlet oxygen, thus generated, is capable of undergoing an ene reaction with typical alkenes such as 2,3-dimethylbut-2-ene and 2-methyl-4,4-dimethylpent-2-ene. The product distribution observed with 1,2-dimethylcyclohexene suggests that the hydroperoxides so obtained are not the result of reaction with ground-state triplet oxygen (Scheme 2).⁹ These observations confirm that one can generate a reactive singlet oxygen within the confines of a zeolite and set the stage for us

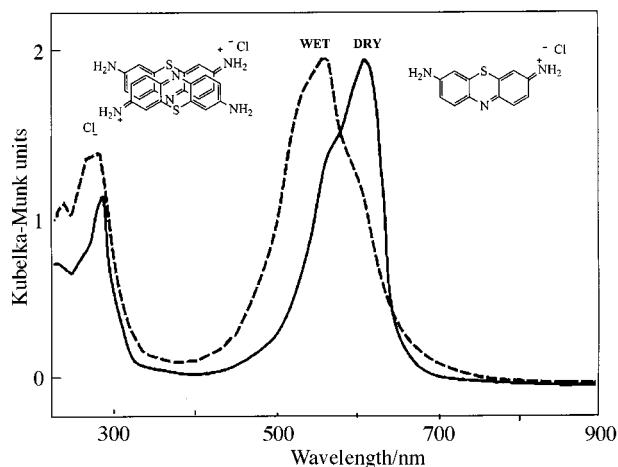
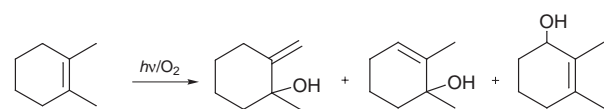
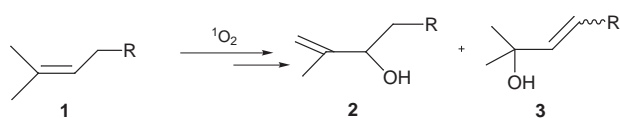


Fig. 2 The diffuse reflectance spectra of thionin included within NaY. The 'dry' and 'wet' samples show different spectra and are differently colored (for colored version of this figure please see <http://www.rsc.org/suppdata/cc/1998/2411>).

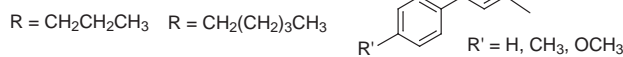


Conditions	Relative Yield (%)		
Rose Bengal / Acetonitrile	89	11	0
Thionin/ NaY/Hexane	90	10	0
Autooxidation	6	39	54

Scheme 2



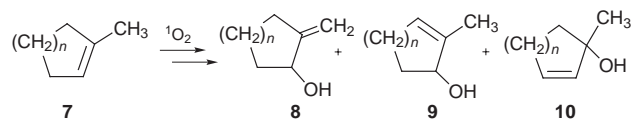
R = CH ₃	Relative Yield (%)	
Thionin/CH ₃ CN	40	60
NaY/Thionin	100	—

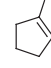
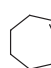


Scheme 3

to explore the initial goal of achieving selectivity during the ene reaction.

A number of alkenes of structure similar to 1-methylpent-2-ene were examined. These alkenes contain two distinct allylic hydrogen atoms and, in an isotropic solution, yield two hydroperoxides with no appreciable selectivity (Scheme 3). Within NaY, a single hydroperoxide is preferentially obtained.^{10,11} Similar selectivity was also observed with related alkenes such as the 1-methyl-4-arylbut-2-enes and even more impressive results were obtained with 1-methylcycloalkenes (Scheme 4).¹⁰ These alkenes yield three hydroperoxides in solution with the hydroperoxide resulting from abstraction of the methyl hydrogens formed in the lowest yield. Surprisingly, the minor isomer in solution was obtained in larger amounts within the zeolite. Thus the selectivity is a characteristic of hydroperoxidation of alkenes within zeolites. Product hydroperoxides were isolated in *ca.* 75% yield. Generally alcohols were more easily extracted out of the zeolite than the hydroperoxides. A number of control experiments ensured that the observed selectivity is not an artifact. The yields reported in the schemes are for alcohols.



		Relative Yield (%)		
	Thionin/CH ₃ CN	6	45	48
	Thionin/NaY/Hexane	100	—	—
	Thionin/CH ₃ CN	10	47	43
	Thionin/NaY/Hexane	100	—	—

Scheme 4

The above selectivity is rationalized on the basis of two independent models.¹¹ In one, the zeolite is postulated to control the conformation of the reactive alkene and, in the other, the zeolite is suggested to polarize the reactive alkene. We wish to emphasize that the above models are only working hypotheses and further experiments are needed (and underway) to identify the origin of selectivity. Formation of both hydroperoxides **2** and **3** from **1** in solution has been rationalized on the basis that singlet oxygen attacks the alkene from the top-right side as shown in Fig. 3 and Scheme 1. In such an approach, the

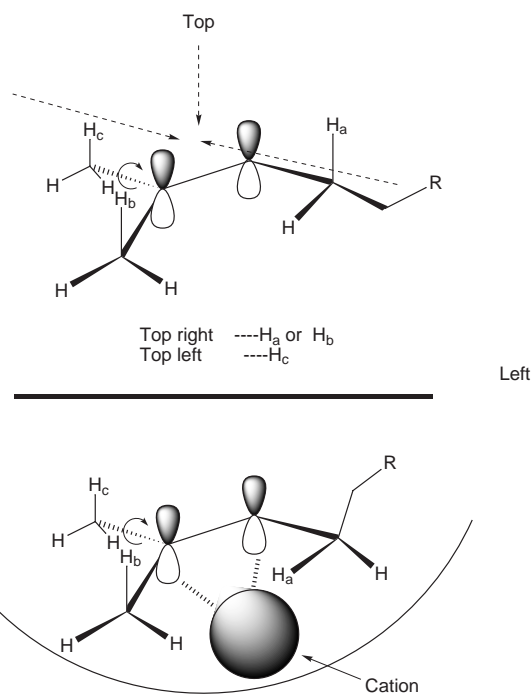


Fig. 3 Cation-alkene interaction within a supercage may control the conformations of allylic hydrogens. For allylic hydrogen abstraction H_a and H_b should be parallel to the π orbital (see top).

transition state is stabilized by secondary interactions between the oxygen and the allylic hydrogens which are situated parallel to the π -p orbitals. In this model, the methyl group on the top-left side (Fig. 3) does not participate in the oxidation process. The results within zeolites clearly suggest that the methylene hydrogens H_a of **1** and **4** (Fig. 3) are not abstracted by the singlet oxygen. While the lack of formation of **3** and **6** within zeolites is an indication that the methylene hydrogens are excluded from the reaction, selective formation of **2** and **5** does not indicate which of the two (or both) methyl groups participates in the oxidation process.

We propose that the R group in the alkene (Fig. 3) plays a crucial role in the type of product(s) formed. While in solution, the most favored conformation places both the methyl and methylene hydrogens in an appropriate geometry for abstraction (Fig. 3), it is quite likely that such a conformation is not favored

within a zeolite. In a supramolecular assembly, one must consider the interactions that arise between the adsorbent/guest and the environment. We speculate that within a zeolite, the alkene will be adsorbed to the surface *via* cation- π interactions. The rotation of the C3-C4 bond may occur under such conditions to relieve the steric strain that develops between the bulky R group and the surface. Such a rotation will place the methylene hydrogens away from the incoming singlet oxygen (Fig. 3), preventing the formation of the tertiary hydroperoxide. The extent of steric repulsion between the surface and the R group may depend on the distance between the group and the surface which, in turn, will be controlled by the size and binding strength of the cation. This model predicts that the selectivity should be directly related to the binding energy of the cation with the alkene; reactions involving larger cations such as Cs⁺ ion may be expected to yield lower selectivity than those involving the smaller Na⁺ ion.

In the second model, the selectivity is attributed to the polarization of the alkene by the interacting cation. As shown in Fig. 4, when the alkene is asymmetric, the interacting cation

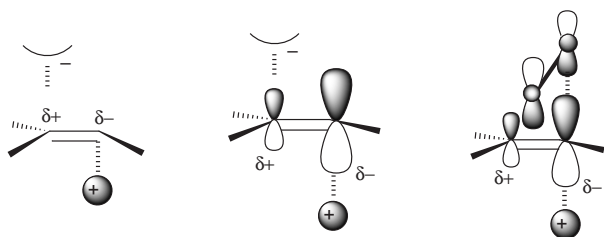


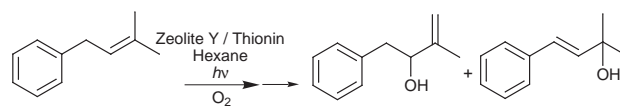
Fig. 4 Cation-alkene interaction may polarize the alkene. Polarization is represented in terms of the size of the orbital.

will be able to polarize the alkene in such a way that the carbon with the greater number of alkyl substituents will bear a partial positive charge (δ^+). Singlet oxygen being electrophilic is expected to attack the less substituted electron rich carbon (δ^-) and lead to an ene reaction in which the hydrogen abstraction occurs selectively from the alkyl group connected to the δ^+ carbon. Polarization of molecules such as pyrene, NO, alkene-oxygen within zeolites has been previously reported.^{12,13} In our system, the extent of polarizability will depend on the charge density of the cation. Smaller cations such as Li⁺ would be expected to polarize the alkene more effectively than larger cations such as Cs⁺. As per this model, selectivity is expected to decrease from Li⁺ to Cs⁺. Consistent with both the above models, the observed selectivity decreases with the size of the cation (Scheme 5; Li⁺ > Na⁺ > K⁺ > Rb⁺ > Cs⁺).¹¹

Both of the above models assume that there is an interaction between the cation and the alkene and that the interaction

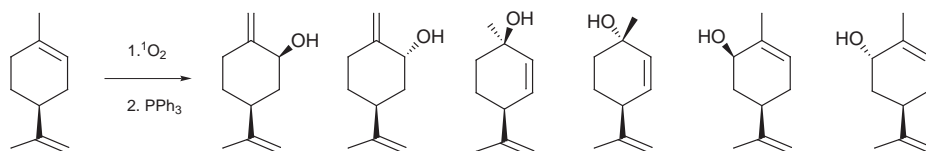
energy decreases with the size of the cation.¹⁴ ²H and double resonance NMR studies are in progress to probe the interaction between the adsorbed alkene and the extra-framework cation. Preliminary *ab initio* quantum mechanical calculations performed with several alkenes clearly show a decreasing trend in the binding energy between the cation and the alkene, the smaller cations binding more strongly.¹⁵ Although at present we have no direct evidence for interaction between cations and alkenes, we have established the existence of such interactions for aromatics *via* absorption, emission and solid state NMR studies.¹⁶ These cation-aromatic interactions, which involve the π -electrons of aromatics, are well established in the literature.¹⁷

Extension of the above oxidation studies to alkenes such as limonene gave a complex mixture (Scheme 6).¹⁸ Control experiments revealed that the alkenes themselves undergo rearrangement prior to oxidation. Careful analysis indicated that the very low concentrations of acidic protons that are present in NaY (<1 per 16 supercages, as determined by NMR and indicator studies described below), a zeolite which is usually considered to be non-acidic, are sufficient to catalyze these rearrangements.¹⁹ Acid catalyzed rearrangement of limonene in solution is well known. In further studies, these very small concentrations of acidic sites were shown to alter the chemistry significantly and to result in a variety of unexpected products that result from the initial protonation of the alkene. We were able to switch off this chemistry, by simply neutralizing the acidic sites with stoichiometric amounts of pyridine. Once these acidic sites are neutralized, oxidation of the alkenes listed in



Cation	Cation radius/Å	Relative Yield (%)	
		2°	3°
LiY / Thionin	0.76	100	—
NaY / Thionin	1.02	85	15
RbY / Thionin	1.52	80	20
CsY / Thionin	1.67	66	34

Scheme 5



Relative Yield (%)

Conditions	A	B	C	D	E	F
Rose Bengal/ CH ₃ CN	20	21	34	10	5	10
NaY/Thionin	Rearrangement— Complex mixture					
NaY/Thionin/ Pyridine	Only					

Scheme 6

Scheme 6 can be readily performed without any side reactions.

A fundamental understanding of both the major reaction mechanisms, and the possible side-reactions, clearly requires a detailed study and quantification of the number of acidic and cation sites present in these materials. Details on the characterization of zeolites for Brønsted acidity are presented in the following section.

Probing M²⁺Y, H⁺Y and M⁺Y zeolites for Brønsted acidity: implications for reactivity

NMR characterization

One of our laboratories has developed and applied a variety of new solid state double resonance NMR methods to probe the acidic sites present in zeolites and to study gas sorption.^{20–24} TRAPDOR NMR methods were used, for example, to probe surface sites which are difficult to observe directly with ²⁷Al MAS NMR methods^{20,22,23} since they are associated with large quadrupole coupling constants. Examples include sites of catalytic interest such as the aluminium atoms associated with the Brønsted acid sites in the zeolite [Si–O(H)–Al] and the Lewis acid sites created by dehydroxylation of the framework or by steaming. The TRAPDOR experiment^{22,25} exploits the dipolar coupling between nearby nuclei to detect the quadrupolar nuclei (²⁷Al) indirectly. Two experiments are performed: in a ¹H–²⁷Al experiment, for example, the first experiment performed is a simple ¹H spin-echo. This is referred to as the control experiment. In the second experiment, a ¹H spin-echo sequence is again performed, but now the quadrupolar nucleus (in this case ²⁷Al) is irradiated for, typically, the evolution period (τ) of the spin-echo. This is shown schematically in Fig. 5.

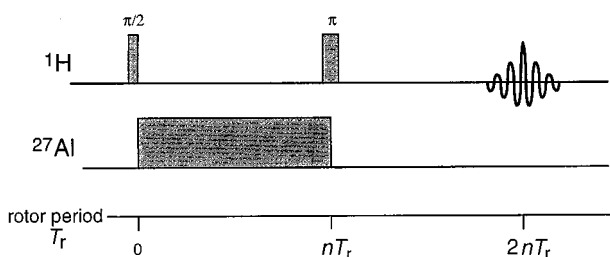
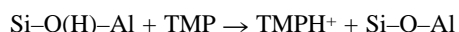


Fig. 5 The ¹H–²⁷Al TRAPDOR NMR sequence. An echo is formed at $2nT_r$, where T_r is the rotor period, nT_r is the evolution period, and n is an integer.

Protons nearby to aluminium spins will no longer be completely refocused, on ²⁷Al irradiation, by the π pulse applied in the middle of this sequence (at nT_r) and their signal, at the echo (at $2nT_r$), will be reduced. This reduction depends on a variety of factors, which include the spinning speeds and ²⁷Al r.f. field strength; more importantly, the loss in signal is extremely sensitive to the ¹H–²⁷Al internuclear distance. This fact can be utilized to assign ¹H resonances to different aluminium-containing species or to probe proximity between different spins. Lewis acid sites are readily detected on absorption of bases such as trimethylphosphine (TMP) or ¹⁵N-labeled monomethylamine: A ³¹P–²⁷Al or ¹⁵N–²⁷Al TRAPDOR NMR experiment is performed and the loss of the ³¹P or ¹⁵N signal at the echo, on ²⁷Al irradiation, indicates that these probe molecules are bound to the Lewis acid site.^{24,25}

A simple probe of acidity involves the reaction of trimethylphosphine (TMP) with the Brønsted acid sites [Si–O(H)–Al]:



Very different chemical shifts are observed for the TMP molecule and TMPH⁺ cations (at *ca.* –67 and –2 ppm, respectively).^{26,23} Since NMR is a quantitative technique, the concentration of Brønsted acid site follows directly from the intensity of the TMPH⁺ resonance. Additional ¹H experiments

have been performed to ensure that complete reaction of the TMP with the Brønsted acid sites occurred. ³¹P–²⁷Al TRAPDOR experiments have also been carried out to assign the ³¹P resonances due to TMP bound to the Lewis acid sites. These methods were applied to characterize HY and CaY.^{27,24}

The ¹H–²⁷Al TRAPDOR NMR spectra of CaY, calcined in an oven at 500 °C, is shown in Fig. 6. The control experiment, (Fig. 6) obtained without ²⁷Al irradiation, shows a number of

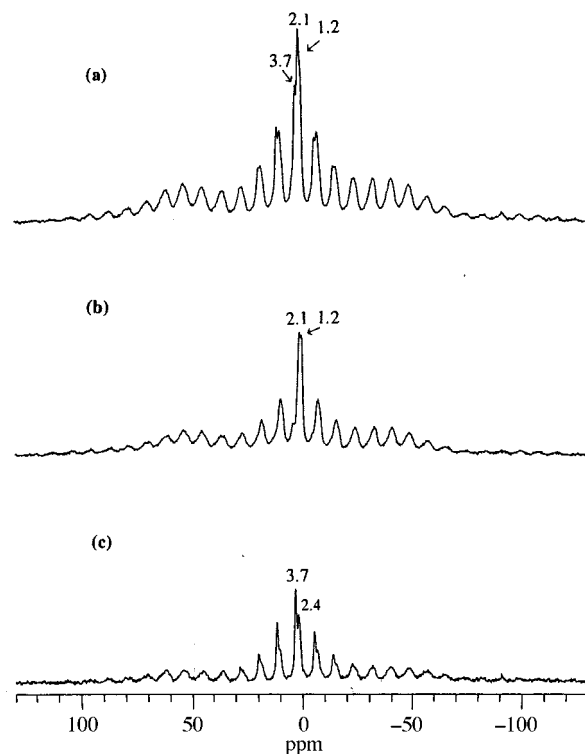


Fig. 6 ¹H–²⁷Al TRAPDOR spectra of CaY-500-oven at –500 °C obtained (a) without and (b) with on-resonance ²⁷Al irradiation during τ ($\tau = 333 \mu\text{s}$, spinning speed = 3 kHz; ²⁷Al r.f. field strength = 55 kHz). The difference spectrum [(a) – (b)] is shown in (c). The intensity of (c) has been scaled by a factor of two with respect to (a) and (b).

different resonances at 3.7, 2.1 and 1.2 ppm. The large spinning sideband manifolds result from residual water that is bound to the calcium cations; (b) shows the spectrum obtained on ²⁷Al irradiation. ¹H resonances that are observed result from proton species that are distant from aluminium atoms, or that are mobile. The difference spectrum shown in (c) contains resonances from proton spins that are nearby to aluminium. The resonance at 3.7 ppm, due to the Brønsted acid sites [Si–O(H)–Al], is observed clearly in this spectrum, consistent with this. The resonance at 2.4 ppm is due to extra framework aluminium hydroxide species created during activation of the zeolite. The large sideband manifolds are visible in (c) indicating that the water molecules are also tightly bound to the zeolite framework. The resonances at 2.1 and 1.2 ppm are assigned to CaOH⁺ and silanol groups, respectively. The CaOH⁺ groups result from the following reaction, which is well established in CaY zeolites, and is a consequence of the large electrostatic field at the divalent cation:²⁸



The observation of Brønsted acid resonances at 3.7 ppm is consistent with this. TMP was sorbed on this material to titrate the acid sites and an estimate of *ca.* 16 Brønsted acid sites per unit cell was obtained for this sample by integrating the TMPH⁺ resonance. ³¹P–²⁷Al TRAPDOR NMR was performed to confirm the lack of Lewis acidity in these samples. Experiments were then carried out for samples activated under a variety of different conditions. CaY activated in an oven at higher temperatures contains less water, but all the other species are

still present. In contrast, CaY activated by slow ramping of the temperature under vacuum to 500, or 600 °C, shows a much lower concentration of Brønsted acid sites (<1 per unit cell, from TMP titration). Again, no evidence for Lewis acidity was observed.

Similar experiments can be used to quantify the number of Brønsted acid sites in HY zeolites.²⁴ Typically, the number is less than the predicted amount from the Si/Al ratio, as some dehydroxylation occurs. The ¹H MAS NMR spectrum of monomethylamine (MMA) sorbed on an HY sample dehydrated at 400 °C under vacuum is shown in Fig. 7, as a function

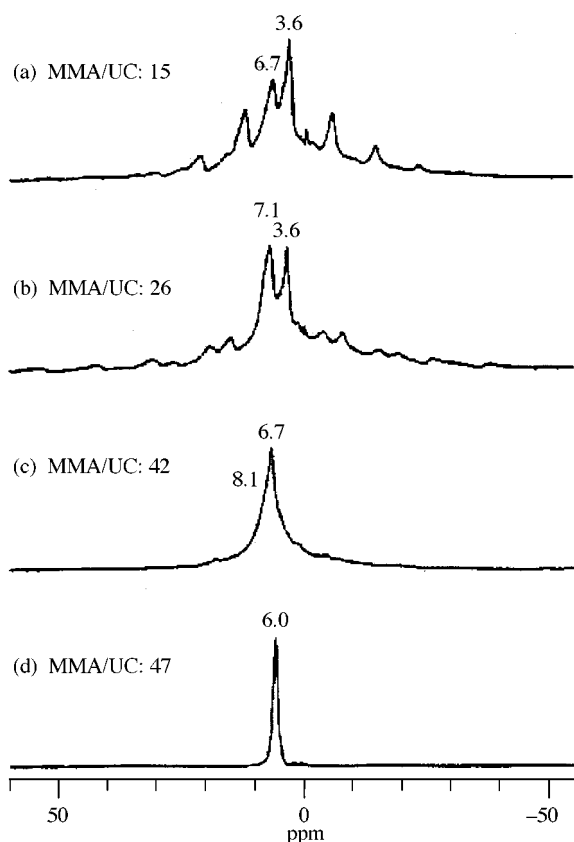


Fig. 7 ¹H MAS NMR spectra of [²H₃]monomethylamine–HY with different loading levels. Loading levels per unit cell are shown on the figure. Spectra were collected at spinning speeds of 3 and 4 kHz for (a) and (b)–(d), respectively. The isotropic resonances are labeled. The small peaks around 0–1 ppm are due to the background signals from the probe head, rotor and inserts. All other resonances are spinning sidebands.

of loading level.²³ Monomethylammonium cations (MMAH⁺) are formed (resonances at 6.7–8.1 ppm), which at temperatures below –40 °C are rigidly bound to the zeolite framework on the ¹H NMR timescale. At loading levels of MMA that exceed the number of Brønsted acid protons (>42 MMA/u.c.), ¹H resonances intermediate in chemical shift between those of MMA (*ca.* 2 ppm) and MMAH⁺ are observed from species undergoing rapid proton transfer reactions between MMA and MMAH⁺. This is seen in (d) where a single resonance at 6.0 ppm is observed. Thus a concentration of between 42 and 47 Brønsted acid sites per unit cell is estimated for this sample. The Brønsted acid concentration, as a function of the dehydration temperature, has also been carefully determined from proton spin counting in ref. 29 and our ¹H MAS NMR results are consistent with this data. Lewis acid sites created as a result of the dehydroxylation process, are clearly observed on TMP or MMA sorption (with ³¹P or ¹⁵N MAS NMR).^{22,23}

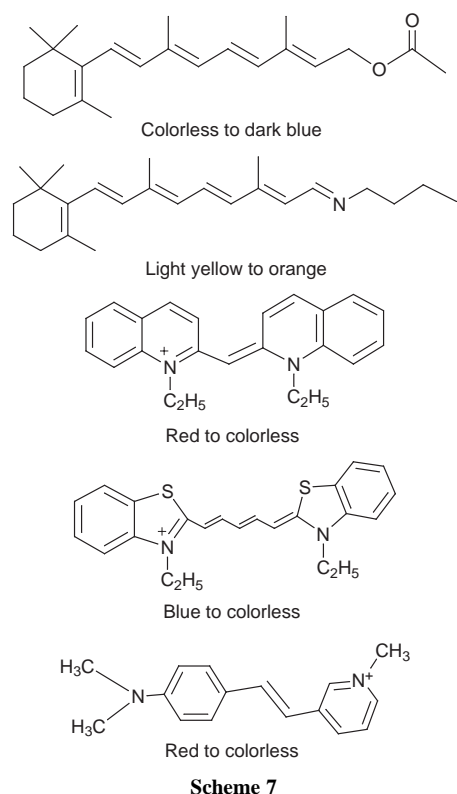
The indicator method

As discussed earlier, thermal reactions of alkenes were observed even within alkali-metal ion-exchanged X and Y zeolites, zeolites not traditionally associated with Brønsted

acidity. The small concentrations of Brønsted acid sites present in these samples are thought to result from cation deficiencies (*i.e.* a M⁺:Al³⁺ ratio of <1) caused by the replacement of M⁺ by H₃O⁺ during ion-exchange or synthesis of the zeolites.^{28,30} Quantification of these Brønsted acid sites was critical in order to rationalize the observed chemistry within M⁺X and M⁺Y zeolites. The materials were initially studied with ¹H MAS NMR with similar methods to those described above.¹⁹ ¹H MAS NMR spectra of activated NaY showed a very weak resonance at 3.6 ppm which could be tentatively assigned to Brønsted acid sites. Its intensity was, however, extremely small in comparison to the intensity of the residual water and the silanol groups and it was difficult to quantify the numbers of Brønsted acid sites per unit cell. TMP was again sorbed on NaY. The ³¹P MAS NMR at –150 °C showed a very weak signal at –2 ppm (1/50 times weaker than the main resonance at –60 ppm from weakly bound/physisorbed TMP, for the sample loaded with 26 molecules per unit cell), which was ascribed to TMPH⁺. From the intensity of this resonance, we estimated that there could be no more than approximately 0.5 Brønsted acid sites per unit cell of NaY. To check the presence of weakly acidic sites, stronger bases such as dimethylamine and methylamine were used as probes for NaY. No evidence for protonation of these probes could be detected with ¹H MAS NMR. Note that when these probe molecules were adsorbed in quantities that exceeded the number of Brønsted acid sites, considerable mobility of the probe molecules was typically observed, indicating rapid exchange of the protons between the probe molecules. Although the exchange process can be frozen out at low temperatures such as –150 °C, this mobility complicates the analysis of spectra obtained for samples with very low concentrations of Brønsted acid sites. Based on these studies it was concluded that the number of Brønsted acid sites within NaY was close to, or beyond, the detection limits of NMR. Therefore, we employed a different technique to detect the acidic sites within zeolites. This involved detecting differences in electronic absorption characteristics between protonated and unprotonated forms of a probe molecule.

The success of this technique depended upon finding a dye molecule that would exhibit different colors under acidic and basic conditions and would easily fit within a zeolite. The set of cyanine dyes that we used is listed in Scheme 7.³¹ All are brightly colored under basic or neutral conditions and turn colorless under acidic conditions. Two dyes, retinol and retinyl acetate, are blue under acidic conditions but are light yellow under basic/neutral conditions. A preliminary test consisted of monitoring the absorption changes upon addition of a small amount (50 to 200 mg) of an activated zeolite to a standard micromolar hexane solution (5 ml) of the dye. When activated NaY was added to a standard solution of retinol or retinyl acetate, the zeolite immediately turned a dark blue color which persisted for nearly an hour. This observation was interpreted as evidence for the presence of Brønsted acidic sites that are strong enough to protonate retinol and retinyl acetate. When the cyanine dye was added to activated NaY, the bright color of the dye faded and the zeolite remained white. Consistent with this, NaX did not show a positive blue test with either retinol or retinyl acetate or with cyanine dyes. This leads us to conclude that NaX is less acidic than NaY.

The number of Brønsted acid sites was estimated by a conventional titration method. Either *n*-butylamine, diethylamine or pyridine was used as a base to quench the acidic sites present in a zeolite. A typical experiment consisted of stirring a known amount of NaY with varying amounts of the base. After at least 6 h of stirring the indicator dye was added and the visible color change was either observed or recorded. Surprisingly when the base was present in amounts more than 1 per 16 cages retinol and retinyl acetate did not become blue and the cyanine dyes maintained their bright colors. This indicated that no more than one acidic site per 16 supercages (*i.e.* 0.5 H⁺ per unit cell)



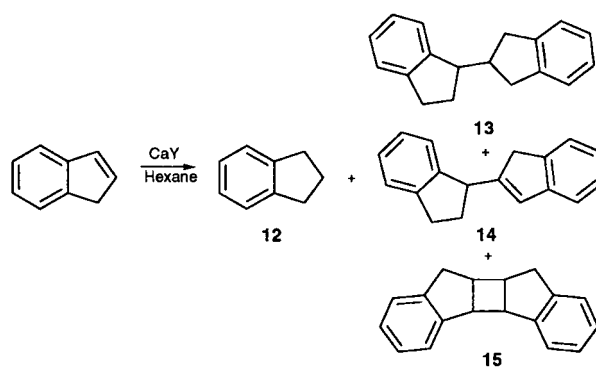
can be present in NaY. Although this number is small, it is large enough to bring about changes in the structure of guest alkenes via a catalytic process.

Careful characterization of CaY, HY, and NaY zeolites has shown that these zeolites contain Brønsted acid sites. Of these HY, as expected, contains the most acidic protons (42–47 per unit cell). This is followed by CaY activated in an oven which contains 16 per unit cell. Even NaY, normally considered to be non-acidic, contain 0.5 protons per unit cell. The acidity of CaY depends on the activation conditions and that of NaY depends on the source. As per our analysis NaX is least acidic. In choosing X and Y zeolites as a reaction media one must be aware of the consequences of the presence of even small numbers of Brønsted acid sites in CaY, HY, and NaY zeolites.^{32–34}

Proton transfer reactions within zeolites

In this section the thermal behavior of three alkenes, indene,³⁵ 4-vinylanisole³⁶ and 1,1-diphenylethylene,³⁷ within CaY is outlined.³⁸ In all cases CaY was activated in an oven at 500 °C; activation at 400 °C under vacuum resulted in a less active zeolite. Inclusion of the alkenes in activated CaY gave brightly colored samples that retained their color for several weeks and, in some cases, even months (see <http://www.rsc.org/suppdata/cc/1998/2411>). For example, 1,1-diphenylethylene gives a green colored zeolite while 4-vinylanisole red–violet and indene dark red. The products isolated, the characterization of the species responsible for the color and a possible mechanism for formation of both the colored species and the final products are described below.

Addition of the activated CaY to a hexane solution of indene resulted in the immediate formation of a dark red color (absorption maximum at 520 nm) that persisted for several months. Extraction of the zeolite with dichloromethane gave products **12–15** (Scheme 8) but, remarkably, did not remove the red color. The red color remained after three months under laboratory conditions and was unaffected by refluxing the zeolite in methanol or water for 24 h or by the addition of dilute HCl. The behavior of vinylanisole was similar to that of indene in that addition of activated CaY to 4-vinylanisole in hexane



gave a vibrant red–violet color. The diffuse reflectance spectrum of the solid zeolite consisted of two broad absorptions at 340 and 580 nm (Fig. 8). The 580 nm absorption was not

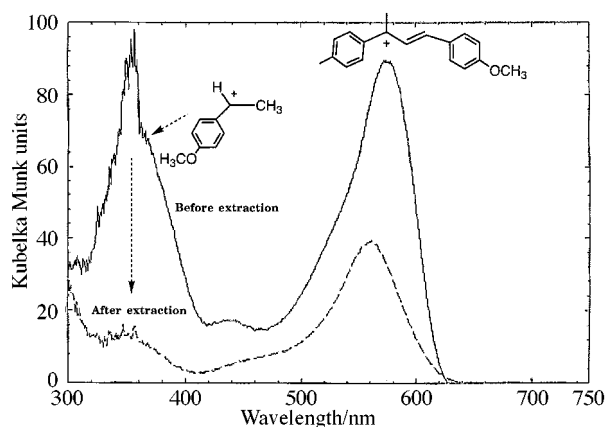
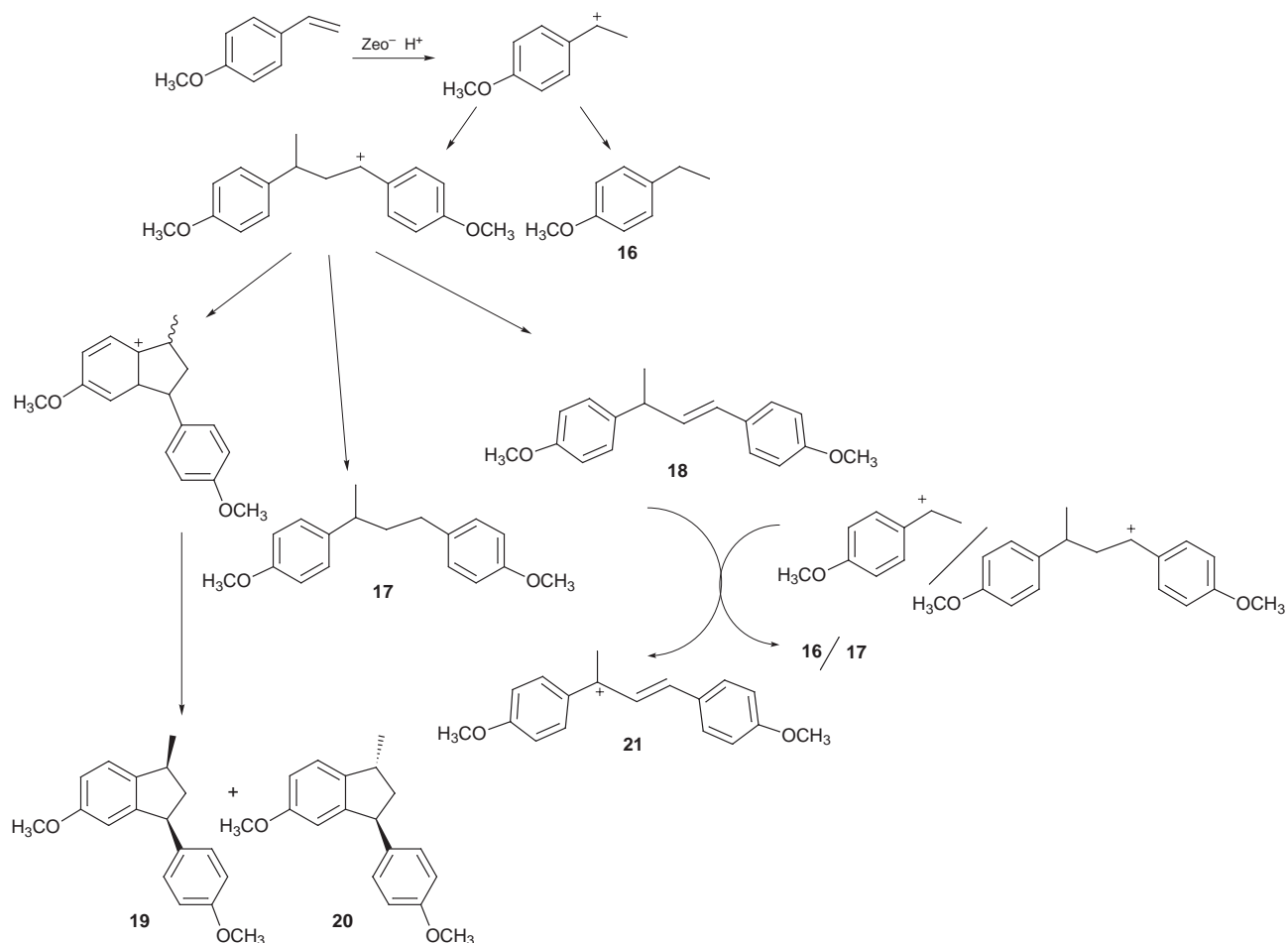


Fig. 8 Diffuse reflectance spectra of 4-vinylanisole included within 500 °C-oven-activated CaY. The sample before extraction shows absorptions due to two independent carbocations. After extraction with dichloromethane, the spectrum is mainly due to the allylic cation (see insert for structure).

removed by any of the extraction procedures noted above for indene. In contrast, extraction of the zeolite with dichloromethane–THF eliminated the 340 nm absorption and gave products **16–20** (Scheme 9). The ratio of the products dependent on the loading level of 4-vinylanisole and on the mode of activation of CaY. Due to lack of space we will not be going into the details on the relationship between the product distribution and loading level. The 340 nm absorption is attributed to the 4-methoxyphenylethyl cation (see insert in Fig. 8), in good agreement with the literature spectrum for this species in solution.³⁹ While this cation has a lifetime of only a few microseconds in solution, it is stable for a few days in the zeolite.

Similarly, addition of CaY to a hexane solution of 1,1-diphenylethylene gave a yellow slurry that turned green and remained so for several days. The diffuse reflectance spectrum (Fig. 9) showed two maxima at 430 and 610 nm. Product extraction (Scheme 10) left a blue zeolite (610 nm). The 430 absorption is attributed to the diphenylmethyl cation, in agreement with the solution spectrum for this species and its independent generation from diphenylethanol in CaY.⁴⁰

The products shown in Schemes 7–9 can be rationalized on the basis of an initial protonation of the olefin by Brønsted acid sites in activated CaY. Detailed H, D isotope studies using D₂O and deuterated extraction solvents were carried out for diphenylethylene and indicated that the first proton comes from acidic sites and the second hydride from the solvent. Scheme 9 illustrates the sequence of reactions that we suggest to explain the formation of the products from 4-vinylanisole; similar schemes can rationalize the products observed for indene and diphenylethylene. A common feature for all three alkenes is the



formation of a strongly colored stable species within CaY. The formation of a red color from indene in the presence of Lewis acids has been reported previously and attributed to carbonium ion **25** (Scheme 11) formed by abstraction of a hydride ion from 2- α -indanylidene **14**.⁴¹ In solution, this cation is only stable for a short time, even under an inert atmosphere. We believe that the 520 nm absorption in CaY is due to the same cation, which is indefinitely stable in the zeolite. Similarly, the red-violet color obtained for 4-vinylanisole is assigned to the allylic cation **21** (Scheme 9). This is consistent with the expected absorption for the 1,3-diphenylpropenyl cation and was confirmed by the independent generation of this species from an alcohol precursor.

While there seems to be general agreement in the literature concerning the structure of the persistent cations from indene and 4-vinylanisole, the origin of the blue color (after extraction to remove the yellow component) from diphenylethylene is not yet resolved. A deep blue or green coloration from diphenylethylene in acidic media (both in solution and on silica-alumina surfaces) has been reported previously and several possible explanations have been suggested (Scheme 12).^{42,43} One of these is the monomer radical cation, although there are conflicting reports on the solution spectrum of the diphenyl-

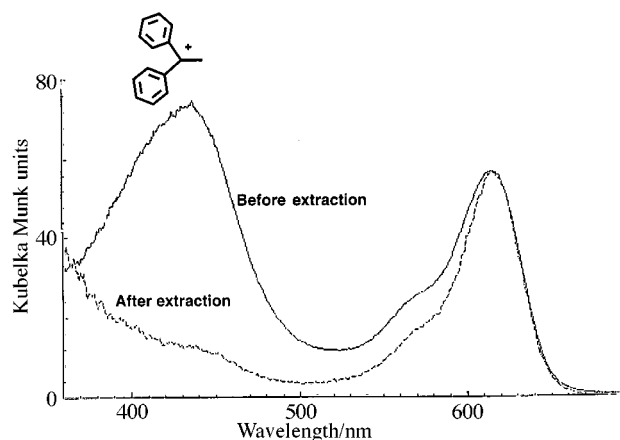
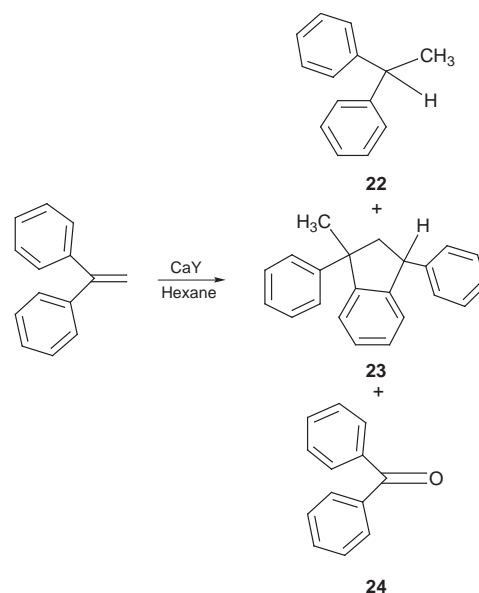
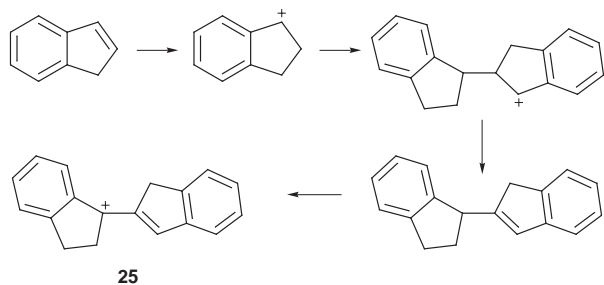
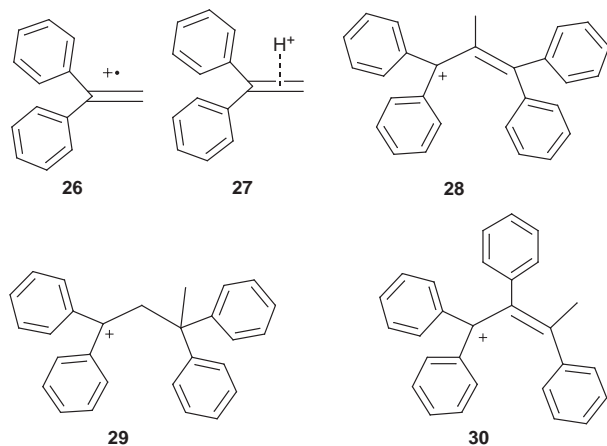


Fig. 9 Diffuse reflectance spectra of diphenylethylene included within 500 °C-oven-activated CaY. The sample before extraction shows absorptions due to two independent carbocations. After extraction with dichloromethane the spectrum is mainly due to an allylic cation.





Scheme 11



Scheme 12

ethylene radical cation. Although we have not been able to record the spectrum for this species in solution, we have obtained spectra for two methyl substituted derivatives. Both the 1,1-diphenylprop-1-ene and 1,1-diphenyl-2-methyl-1-ene radical cations have absorption maxima at *ca.* 400 nm with a weak absorption at >700 nm (Fig. 10). We expect the

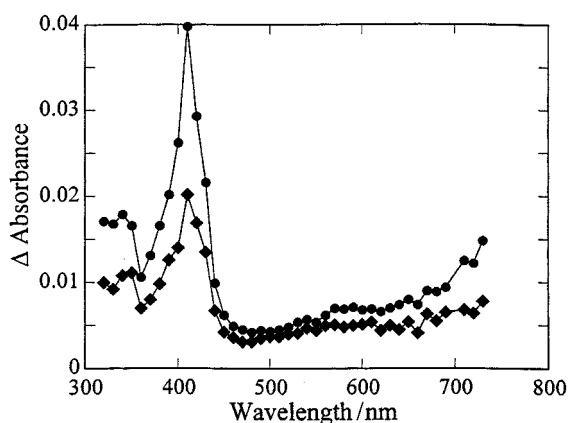


Fig. 10 Transient absorption spectra of the 1,1-diphenyl-2-methylprop-1-ene radical cation generated by 9,10-dicyanoanthracene/biphenyl sensitization in acetonitrile (●, 0.7 μ s after laser excitation; ◆, 1.8 μ s).

diphenylethylene radical cation to absorb in the same region, making it unlikely that the blue species in CaY is the monomer radical cation. An alternate assignment for the colored species is an olefin-acid π -complex,⁴²ⁱ although this proposal has not received much experimental support. Others have suggested dimeric cations such as **28** or **29**; of these **29** is less likely to absorb above 600 nm. In fact generation of this species from alkene **32** gave an absorption identical to that of diphenylmethyl cation. Therefore, the original suggestion **28** by Rooney and Hathaway⁴³ is still one of the most likely structures for the blue colored species; we believe that **30** is also a reasonable possibility.

The difficulty in assigning a structure to the blue species obtained from diphenylethylene arises from the fact that a stable

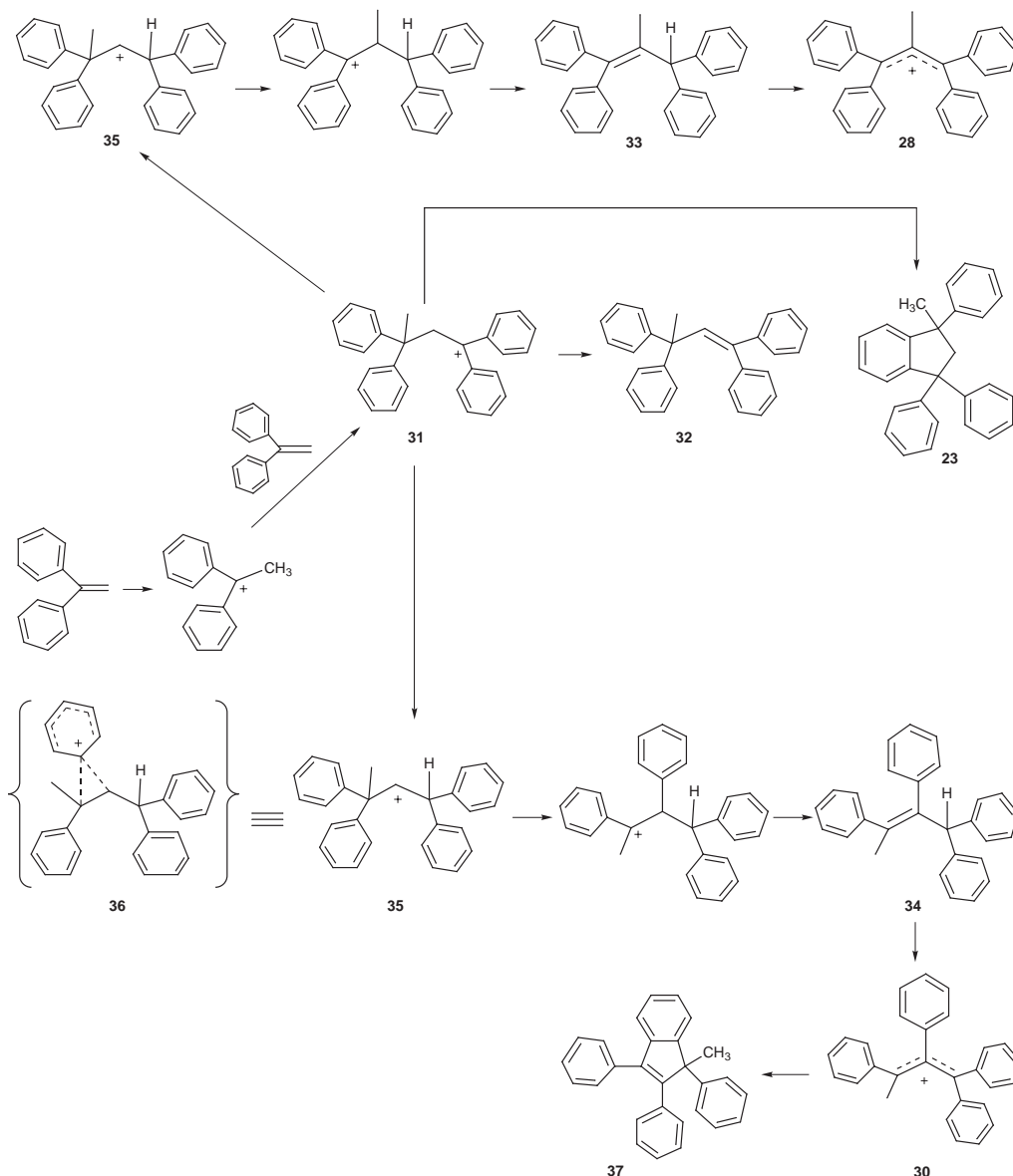
dimeric alkene, that is also a good hydrogen donor, has not been isolated, unlike the results for indene and 4-vinylanisole. As shown in Scheme 13, the only alkene that can be formed from the dimeric cation **31** is **32**, which has no hydrogen that can be easily removed as a hydride. However, alkenes **33** and **34** (Scheme 13) are good hydrogen donors and can give cations **28** and **30** by a similar mechanism to that shown in Schemes 9 and 11. These cations would be expected to absorb above 600 nm. The two alkenes (**33** and **34**) can be formed by rearrangement of **31** to a less stable classical cation **35**. In the absence of other competing processes, even this relatively unlikely rearrangement may occur within a zeolite. In fact if one views **35** as a non-classical phenonium ion (**36** in Scheme 13), rearrangement of **31** to **36** appears feasible. Alkenes **33** and **34** may be formed from **35** via migration of either a methyl or phenyl group as illustrated in Scheme 13. Thus, we believe that the colored species formed from diphenylethylene within CaY is either **28** or **30**. We are currently synthesizing precursors of these cations for studies of their absorption spectra within zeolites.

The extraordinary stability of the carbocations **21**, **25** and **28/30** derives partly from the π -conjugation with the aromatic substituents. This kinetic stability must be augmented by the highly polar nature of the zeolite supercage. In all these systems, the cations that are generated serve as a counter ion for the zeolite framework and thus become part of the zeolite structure. The unusual ability to stabilize certain carbocations within zeolites has allowed us to handle them as 'normal' laboratory chemicals. For example we have been able to record emission from several of these cations. One such example is provided in Fig. 11. The technique of stabilizing reactive intermediates within the structures of zeolite should allow us characterize, in the future, the excited state properties of reactive intermediates such as carbocations and radical cations.⁴⁴

Electron transfer within zeolites

Electron transfer within zeolites has been the subject of investigation for several decades. Some studies have involved spontaneous electron transfer in which the guest, upon inclusion within an activated zeolite, transfers an electron to the zeolite to form a stable radical cation. Stamires and Turkevich were the first to observe spontaneous electron transfer between the host NH_4^+Y zeolite and the guests 1,1-diphenylethylene, triphenylamine, quinoline, perylene, aniline and *p*-phenylene diamine.⁴⁵ We have generated and stabilized radical ions from a number of polyenes and oligomers of thiophenes.⁴⁶ For example, when activated Na-ZSM-5 (Si/Al = 23) was stirred with α,ω -diphenylpolyenes (*trans*-stilbene, diphenylbutadiene, diphenylhexatriene, diphenyloctatetraene, diphenyldecapentaene, and diphenyldodecahexaene) in 2,2,4-trimethylpentane, the initially white zeolite and colorless to a pale yellow olefins were transformed into highly colored solid complexes within a few minutes. The samples all exhibited intense EPR signals with *g* values of 2.0028. Diffuse reflectance spectra of these powders (Fig. 12) were identical to the spectra of the radical cations of a few α,ω -diphenylpolyenes reported in the literature.⁴⁷ Diffuse reflectance and EPR results favor the conclusion that the colored species formed upon inclusion of α,ω -diphenylpolyenes in Na-ZSM-5 are radical cations. The radical ions thus generated were unusually long lived (several months). The exact nature of the electron acceptor within the zeolite had yet to be unequivocally identified. Although spontaneous generation of radical cations has been established for a number of substrates within Na-ZSM-5 and HY, similar results have not been reported within NaX and NaY zeolites.⁴⁸

In addition to spontaneous electron transfer, relatively long-lived radical cations (lifetimes of milli- to micro-seconds) can be readily generated by direct laser excitation of a variety of aromatic substrates within X and Y zeolites. This phenomenon was originally reported by Iu and Thomas with NaY and NaX



Scheme 13

zeolites as the acceptors and pyrene and anthracene as the donors.⁴⁹ Our recent results demonstrate that direct excitation of aryl and diarylethylenes in zeolites also leads to radical cation formation, in competition with other excited state decay processes. For example, diffuse reflectance laser flash photolysis of *trans*-stilbene included in NaX zeolite leads to the

formation of transient signals assigned to the *trans*-stilbene radical cation (475 nm) and zeolite trapped electrons (Na_4^{3+} , 500 nm).^{50,51} The latter can be removed by purging the samples with oxygen, leading to the unambiguous characterization of the radical cation. The *trans*-stilbene radical cation was also

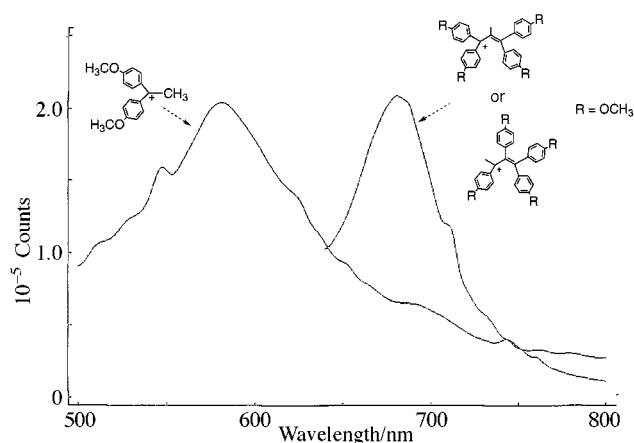


Fig. 11 Fluorescence emission from two cations trapped within CaY. Possible structures of the cations are also shown.

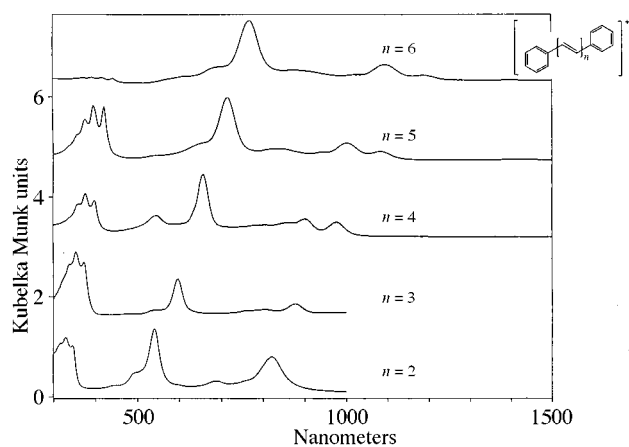
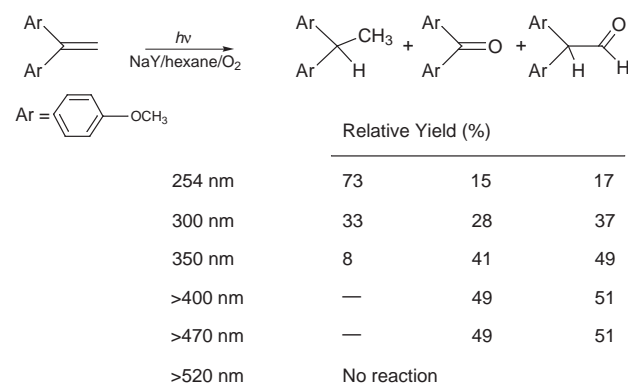


Fig. 12 Diffuse reflectance spectra of α,ω -diphenylpolyenes included within Na-ZSM-5 ($\text{Si}/\text{Al} = 23$). The absorption is due to stabilized radical cations of the alkanes.

observed upon excitation of *cis*-stilbene, in addition to weak signals due to photocyclization to give dihydrophenanthrene. There was no evidence for the generation of the *cis* radical cation (510 nm). However, a mixture of *cis* and *trans* radical cations was observed upon excitation of the *cis*-stilbene/tetranitromethane charge transfer complex in NaX zeolite, providing evidence that both radical cations were stable with respect to isomerization on the timescale of the laser experiments. Product studies carried out with laser irradiation demonstrated that substantial *cis*–*trans* isomerization of stilbene occurred within a few laser pulses. The combined results lead to the conclusion that *cis*–*trans* isomerization followed by photoionization of *trans*-stilbene was responsible for the observation of the *trans* radical cation upon excitation of *cis*-stilbene. We believe that an alternative possibility of photochemical isomerization within the laser pulse is less likely. The less efficient photoionization of *cis*-stilbene was consistent with its shorter singlet lifetime and the fact that it has an additional decay pathway involving photocyclization.

Direct excitation of 4-vinylanisole and *trans*-anethole,⁵² as well as several other styrenes,⁵³ in zeolites also leads to the formation of the respective radical cations. For example, the *trans*-anethole radical cation has two characteristic absorption bands at 620 and 390 nm that agree well with the spectra for the same species in solution. Similar experiments using direct excitation of a number of di(4-methoxyphenyl)ethylenes in NaX zeolites provided evidence for formation of trapped electrons, indicating that photoionization also occurs for these alkenes.⁵⁴ However, the yields were considerably lower than for the styrenes, making it difficult to characterize the radical cations.

The products of direct excitation of a hexane slurry of di(4-methoxyphenyl)ethylene included within NaY zeolite are shown in Scheme 14.⁵⁵ Interestingly, no products are formed in



Scheme 14

the absence of oxygen and the nature of the products depends on the excitation wavelength (Scheme 14). The key intermediate in both the reduction and the oxidation processes is believed to be the radical cation of di(4-methoxyphenyl)ethylene. The absorbing species during short and long wavelength excitations are thought to be different: at long wavelength it is in the alkene–oxygen complex and at short wavelength the uncomplexed alkene. The formation of hydrocarbon–oxygen complexes within zeolites had been extensively investigated by Frei *et al.*⁵⁶ The diffuse reflectance spectra shown in Fig. 13 indicate that di(4-methoxyphenyl)ethylene forms an oxygen complex when present within NaY. A proposed mechanism for the formation of products upon short and long wavelength excitations is shown in Scheme 15. Under both conditions an electron transfer is thought to be the primary step. During short wavelength excitation the primary electron acceptor is presumed to be the zeolite and during the long wavelength excitation the oxygen complexed to the alkene is likely the electron acceptor. Experiments aimed at a more detailed understanding of these reactions are in progress.

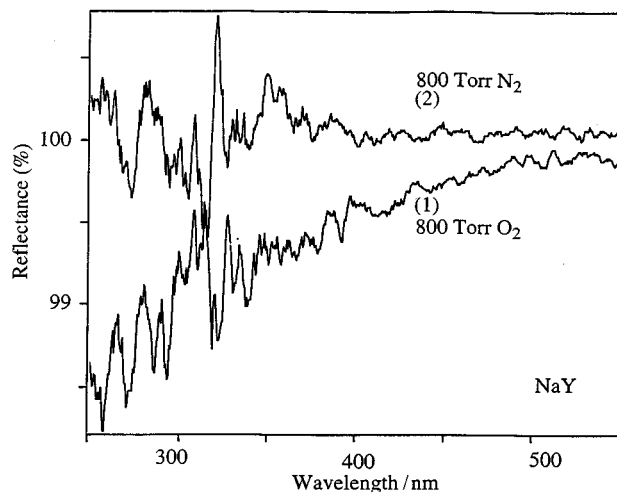
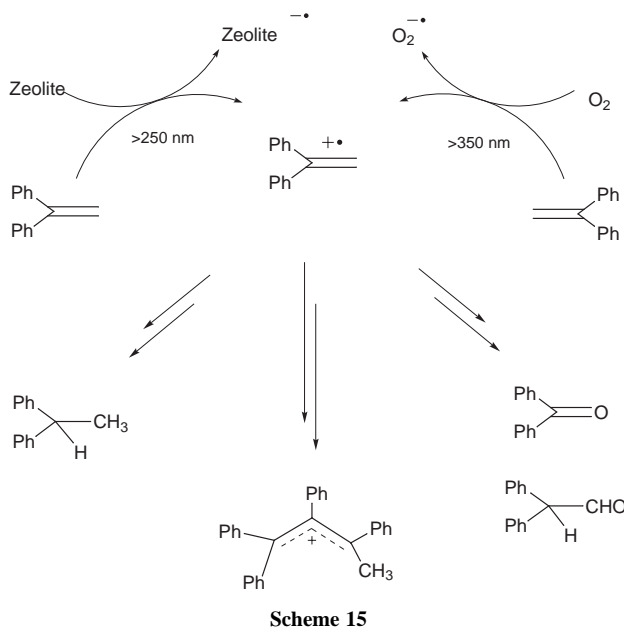


Fig. 13 Diffuse reflectance spectra of 4,4'-dimethoxydiphenylethylene included within NaY. Trace (1) is the difference of spectra taken after and before loading 800 Torr oxygen into the room temperature zeolite. Trace (2) is a control spectrum in which nitrogen was loaded instead of oxygen. Oxygen shows an absorption extending to 500 nm whereas nitrogen shows no such absorption. (We thank S. Vasenkov and H. Frei, University of California, Berkeley for recording the spectra for us).



Scheme 15

The stabilization of organic radical cations within zeolites suggests that the confined interior space of a zeolite should provide an ideal environment for carrying out photosensitized electron transfer reactions. This approach has advantages in that one does not require prior preparation of an activated zeolite which may have a relatively small number of active sites as in the spontaneous electron transfer. Photosensitized electron transfer should also be applicable to a wider range of substrates. In addition, the zeolite environment promotes charge separation which is expected to be advantageous, since it will reduce the rate of the back-electron-transfer process that decreases the efficiency of these reactions in solution. We have used the dimerization of arylalkenes to demonstrate the viability of carrying out photoinduced electron transfer reactions for independently loaded sensitizers and alkene donors and to examine the effect of the zeolite environment on the product selectivity. The results obtained for *trans*-anethole using 2,3-dicyanonaphthalene and 9-cyanoanthracene as sensitizers are typical. For example, a combination of steady state and time-resolved fluorescence measurements indicated that the singlet excited state of the sensitizer was quenched by the alkene, predominantly *via* a static mechanism. Diffuse re-

flectance flash photolysis experiments were carried out using 355 nm excitation which excited the sensitizer only. The results demonstrated that the efficient singlet quenching of the sensitizer was accompanied by formation of the *trans*-anethole radical cation (Fig. 14). The latter has a spectrum similar to that

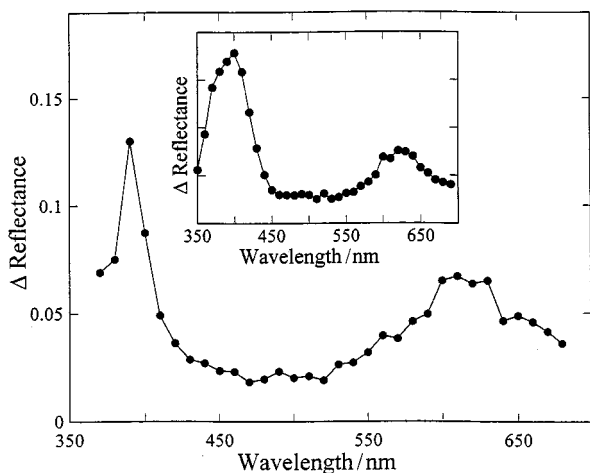


Fig. 14 Transient spectra measured after 355 nm excitation of 2,3-dicyano-naphthalene plus *trans*-anethole in NaX. The inset shows the spectrum obtained by direct 266 nm excitation of *trans*-anethole in NaX.

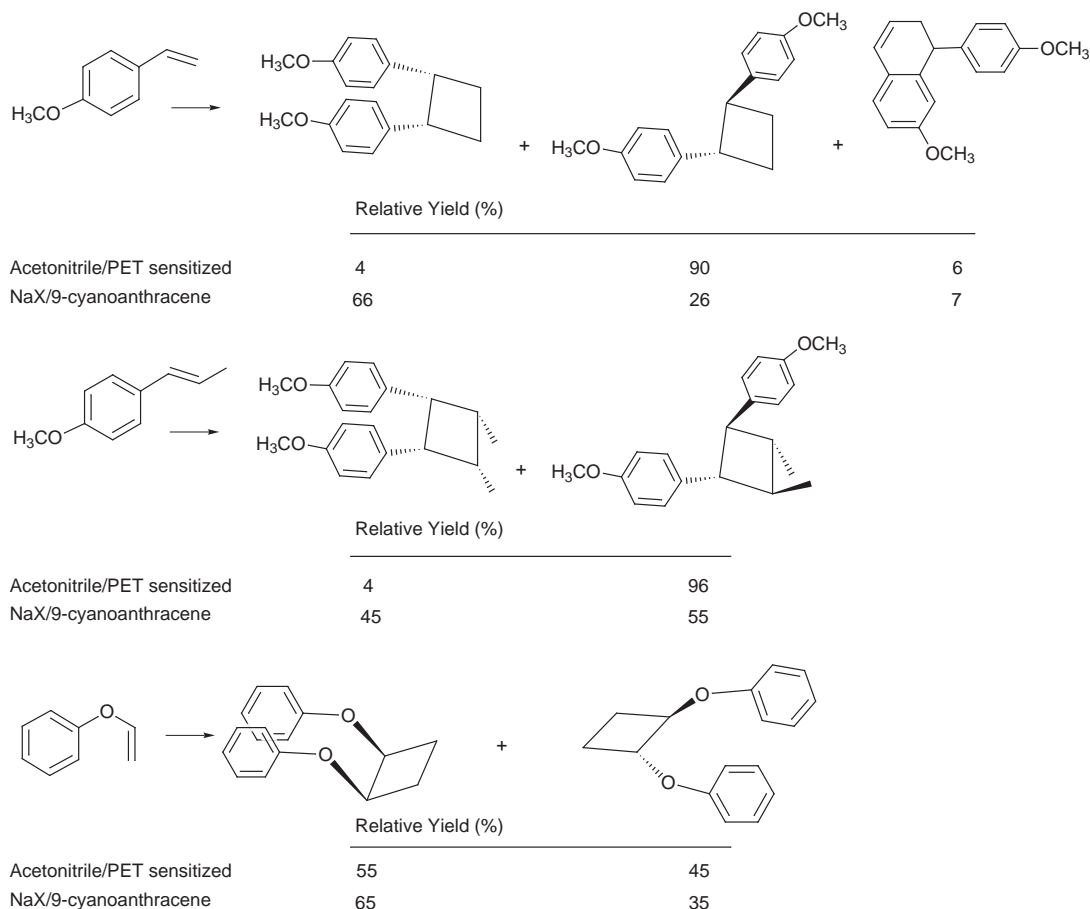
obtained by direct excitation of *trans*-anethole at 266 nm. The transient spectra also provided evidence for photoionization of the cyanoaromatic sensitizers in competition with electron transfer quenching in the zeolite environment. Efficient electron transfer was observed for 9-cyanoanthracene and 1-cyano-naphthalene sensitizers with *trans*-anethole and 4-vinylanisole, demonstrating the generality of these results. In each case the radical cation was relatively long-lived, illustrating the potential

of the zeolite environment for overcoming the limitation of back electron transfer.

The products of the radical cation initiated dimerization of a series of arylalkenes with cyanoaromatic and quinolinium and acridinium sensitizers were examined. The results indicate that the radical cations add to the precursor alkenes to give dimeric products (Scheme 16), as has been observed in solution. In some cases oxidation of the alkenes accompanied dimer formation. A number of control experiments were carried out to ensure that the observed products resulted from sensitization rather than direct photolysis of the alkenes and to ensure that the product ratios did not reflect further reactions of the initial dimers. The product studies demonstrated that radical cation mediated dimerization occurred readily in the zeolite environment and suggested that the radical cations observed in the transient experiments are reactive. The dimer ratios also illustrated some important differences between the solution and zeolite chemistry. For example, although both *cis/syn* and *trans/anti* dimers were formed, the zeolite favors the *cis/syn* product which has a more spherical shape that is similar to the geometry of the supercage. We believe that this reflects the fact that the more linear *trans/anti* isomers are best accommodated in two supercages whereas the *cis/syn* dimer can be formed within a single cage and therefore its formation is the more favorable process. It also appears that the zeolite environment is more important in determining the geometry of the dimeric products than the method (direct or sensitized photocycloaddition *vs.* radical ion initiation) used for their generation.

Concluding remarks

The chemistry of alkenes in zeolites illustrates both the potential complexity and utility of zeolites as reaction media. For example, the results discussed above demonstrate that spontaneous thermal proton and electron transfer reactions are



Scheme 16

common, particularly for zeolites with relatively large numbers of active sites. NMR studies are particularly useful in correlating the number and type of active sites with the chemistry observed and permit one to select a zeolite and an activation procedure that can be used to tune the chemistry. In cases where the zeolite contains fewer active sites, stable alkenes can undergo a range of photochemical reactions, as demonstrated with the energy transfer sensitized singlet oxygen ene reaction and photoinduced electron transfer reactions that lead to dimeric products. Both examples serve to illustrate the ease with which bimolecular reactions between independently loaded donors and acceptors in zeolites can be carried out. A combination of techniques, including product studies, fluorescence and diffuse reflectance flash photolysis, can provide a detailed picture of the reactive intermediates that lead to the observed chemistry. Of particular interest are the changes in product selectivity that result from carrying out these reactions in the constrained space of the zeolite cavity. The results discussed herein provide an excellent basis for the development of sufficient predictive power that one can tune the behavior of the thermal and photochemical behavior for substrates within zeolites in order to achieve a desired product outcome.

Acknowledgments

V. R. thanks the Division of Chemical Sciences, Office of Basic Energy Sciences, Office of Energy Research, US Department of Energy for generous support of this program and K. Pitchumani, K. J. Thomas, V. Jayathirtha Rao, J. Shailaja, R. J. Robbins and X. Li for their contributions to the work presented here. C. P. G. acknowledges the Donors of the Petroleum Research Fund, administered by the American Chemical Society, and the National Science Foundation National Young Investigator program (DMR-9458017) for support of this research and Hsien-Ming Kao for experimental and intellectual contributions towards the results presented here. L. J. J. thanks L. Brancaloni, D. Brousmiche and P. D. Wood for their contributions to the work presented here.

Notes and References

- K. Kalyanasundaram, *Photochemistry in Microheterogeneous Systems*, Academic Press, New York, 1987; *Photochemistry in Organized and Constrained Media*, ed. V. Ramamurthy, VCH, New York, 1991.
- D. W. Breck, *Zeolite Molecular Sieves: Structure, Chemistry and Use*, Wiley, New York, 1974; A. Dyer, *An Introduction to Zeolite Molecular Sieves*, Wiley, Bath, UK, 1988.
- N. J. Turro and M. Garcia-Garibay in *Photochemistry in Organized and Constrained Media*, ed. V. Ramamurthy, VCH, New York, 1991, p. 1; N. J. Turro, in *Inclusion Phenomena and Molecular Recognition*, ed. J. Atwood, Plenum Press, New York, 1990, p. 289.
- W. J. Mortier, *Compilation of Extra Framework Sites in Zeolites*, Butterworth Scientific Ltd, Guildford, UK, 1982.
- C. P. Grey, F. I. Poshni, A. Gualtieri, P. Norby, J. C. Hanson and D. R. Corbin, *J. Am. Chem. Soc.*, 1997, **119**, 1981.
- Singlet Oxygen*, ed. H. H. Wasserman and R. W. Murray, Academic Press, New York, 1979; *Singlet Oxygen*, ed. A. A. Frimer, CRC Press: Boca Raton, 1985, vol. 1-4.
- M. Prein and W. Adam, *Angew Chem., Int. Ed., Engl.*, 1996, **35**, 477.
- V. Ramamurthy, D. R. Sanderson and D. F. Eaton, *J. Am. Chem. Soc.*, 1993, **115**, 10 438.
- C. S. Foote, *Acc. Chem. Res.*, 1968, **1**, 104.
- X. Li and V. Ramamurthy, *J. Am. Chem. Soc.*, 1996, **118**, 10 666.
- R. Robbins and V. Ramamurthy, *Chem. Commun.*, 1997, 1071.
- P. H. Kasai and R. J. Bishop, Jr., *J. Am. Chem. Soc.*, 1972, **94**, 5560; P. H. Kasai and R. J. Bishop, Jr., *J. Phys. Chem.*, 1973, **77**, 2308.
- V. Ramamurthy and D. R. Sanderson, *J. Phys. Chem.*, 1993, **97**, 13 380.
- R. H. Staley and J. L. Beauchamp, *J. Am. Chem. Soc.*, 1975, **97**, 5920; J. Sunner, K. Nishizawa and P. Kebarle, *J. Phys. Chem.*, 1981, **85**, 1814; C. Schade and P. v. R. Schleyer, *Adv. Organomet. Chem.*, 1987, **27**, 169; W. Setzer and P. v. R. Schleyer, *Adv. Organomet. Chem.*, 1985, **24**, 353.
- J. Chandrasekar and B. Sunoj, unpublished results; work in progress.
- V. Ramamurthy, J. V. Caspar, D. F. Eaton, E. W. Kuo and D. R. Corbin, *J. Am. Chem. Soc.*, 1992, **114**, 3882; V. Ramamurthy, J. V. Caspar, D. R. Corbin, B. D. Schlyer and A. H. Maki, *J. Phys. Chem.*, 1990, **94**, 3391; M. A. Hepp, V. Ramamurthy, D. R. Corbin and C. Dybowski, *J. Phys. Chem.*, 1996, **96**, 2629.
- A. N. Fitch, H. Jobic and A. Renouprez, *J. Phys. Chem.*, 1986, **90**, 1311; A. N. Fitch, H. Jobic and A. Renouprez, *J. Phys. Chem.*, 1986, **90**, 1311; M. Czjzek, T. Vogt and H. Fuess, *Angew. Chem., Int. Ed. Engl.*, 1989, **28**, 770; C. Mellot, M. H. Simonot-Grange, E. Pilverdier, J. P. Bellat and D. Espinat, *Langmuir*, 1995, **11**, 1726; M. Czjzek, T. Vogt and H. Fuess, *Zeolites*, 1992, **12**, 237; C. Kirschhock and H. Fuess, *Zeolites*, 1996, **17**, 381; R. Goyal, A. N. Fitch and H. Jobic, *J. Chem. Soc., Chem. Commun.*, 1990, 1152.
- R. J. Robbins and V. Ramamurthy, unpublished results.
- V. Jayathirtha Rao, D. L. Perlstein, R. J. Robbins, P. H. Lakshminarasimhan, H.-M. Kao, C. P. Grey and V. Ramamurthy, *Chem. Commun.*, 1998, 269.
- C. P. Grey and A. J. Vega, *J. Am. Chem. Soc.*, 1995, **117**, 8232.
- C. P. Grey and B. S. A. Kumar, *J. Am. Chem. Soc.*, 1995, **117**, 9071.
- H.-M. Kao and C. P. Grey, *J. Phys. Chem.*, 1996, **100**, 5105.
- H. M. Kao and C. P. Grey, *Chem. Phys. Lett.*, 1996, **259**, 459.
- H. M. Kao and C. P. Grey, *J. Am. Chem. Soc.*, 1997, **119**, 627.
- C. P. Grey, A. J. Vega and W. S. Veeman, *J. Chem. Phys.*, 1993, **98**, 7711.
- W. P. Rothwell, W. Chen and J. H. Lunsford, *J. Am. Chem. Soc.*, 1984, **106**, 2452; J. H. Lunsford, W. P. Rothwell and W. Shen, *J. Am. Chem. Soc.*, 1985, **107**, 1540.
- H.-M. Kao, C. P. Grey, K. Pitchumani, P. H. Lakshminarasimhan and V. Ramamurthy, *J. Phys. Chem.*, 1998, **102**, 5627.
- J. W. Ward, *J. Catal.*, 1968, **10**, 34.
- Z. Luz and A. J. Vega, *J. Phys. Chem.*, 1987, **91**, 365.
- D. W. Breck, *Zeolite Molecular Sieves: Structure, Chemistry and Use*, Wiley, New York, 1974, p. 461.
- K. J. Thomas and V. Ramamurthy, *Langmuir*, in press.
- Recently, there have been reports in which photochemical reactions of alkenes in H⁺ zeolites have been investigated.³³ However, it has been our experience that alkenes undergo Brønsted acid catalyzed reaction in H⁺Y zeolites.³⁴ Therefore, H⁺ zeolites should be avoided as hosts when investigating the photochemical behavior of alkenes.
- V. Fornes, H. Garcia, M. A. Miranda, F. Mojarrad, M. J. Sabater and N. N. E. Suliman, *Tetrahedron*, 1996, **52**, 7755; M. L. Cano, A. Corma, V. Fornes, H. Garcia, M. A. Miranda, C. Baerlocher and C. Lengauer, *J. Am. Chem. Soc.*, 1996, **118**, 11006; A. Corma, H. Garcia, M. A. Miranda, J. Primo and M. J. Sabater, *J. Am. Chem. Soc.*, 1994, **116**, 2276.
- P. H. Lakshminarasimhan, and V. Ramamurthy, unpublished results; M. Kojima, H. Takeya, Y. Kurovama and S. Oishi, *Chem. Lett.*, 1997, 997.
- K. Pitchumani and V. Ramamurthy, *Chem. Commun.*, 1996, 2763.
- V. Jayathirtha Rao, N. Prevost, V. Ramamurthy, M. Kojima and L. J. Johnston, *Chem. Commun.*, 1997, 2209.
- K. Pitchumani, P. H. Lakshminarasimhan, N. Prevost, D. R. Corbin and V. Ramamurthy, *Chem. Commun.*, 1997, 181.
- K. Pitchumani, A. Joy, N. Prevost and V. Ramamurthy, *Chem. Commun.*, 1997, 127; K. Pitchumani, P. H. Lakshminarasimhan, G. Turner, M. G. Bakker, and V. Ramamurthy, *Tetrahedron Lett.*, 1997, 371; K. Pitchumani, D. R. Corbin and V. Ramamurthy, *J. Am. Chem. Soc.*, 1996, **118**, 8152.
- R. A. McClelland, C. Chan, F. Cozens, A. Modro and S. Steenken, *Angew. Chem., Int. Ed. Engl.*, 1991, **30**, 1337.
- R. A. McClelland, V. M. Kangasabapathy and S. Steenken, *J. Am. Chem. Soc.*, 1988, **110**, 6913; A. Azarani, A. B. Berinstain, L. J. Johnston and S. Kazanis, *J. Photochem. A: Chem.*, 1991, **57**, 175.
- H. J. Prosser and R. N. Young, *Eur. Polym. J.*, 1972, **3**, 879.
- H. P. Leftin and W. K. Hall, *J. Phys. Chem.*, 1960, **64**, 382; H. P. Leftin, *J. Phys. Chem.*, 1960, **64**, 1714; H. P. Leftin and W. K. Hall, *J. Phys. Chem.*, 1962, **66**, 1457; H. P. Leftin, M. C. Hobson and J. S. Leigh, *J. Phys. Chem.*, 1962, **66**, 1214; J. J. Rooney and R. C. Pink, *Trans. Faraday Soc.*, 1962, 1632; W. K. Hall, *J. Catal.*, 1962, **1**, 53; F. R. Dollish and W. K. Hall, *J. Phys. Chem.*, 1965, **69**, 4402; V. Fornes, H. Garcia, S. Jovanic and V. Marti, *Tetrahedron*, 1997, **53**, 4715; A. Evans, P. M. S. Jones and J. H. Thomas, *J. Chem. Soc.*, 1957, 104.
- J. J. Rooney and B. J. Hathaway, *J. Catal.*, 1964, **3**, 447.
- M. K. Boyd, in *Molecular and Supramolecular Photochemistry*, ed. V. Ramamurthy and K. S. Schanze, Marcel Dekker, New York, 1997, vol. 1, p. 147; L. J. Johnston, *Chem. Rev.*, 1993, **93**, 251.
- D. N. Stamires and J. Turkevich, *J. Am. Chem. Soc.*, 1964, **86**, 749.
- V. Ramamurthy, J. V. Caspar and D. R. Corbin, *J. Am. Chem. Soc.*, 1991, **113**, 594; J. V. Caspar, V. Ramamurthy and D. R. Corbin, *J. Am. Chem. Soc.*, 1991, **113**, 600.

- 47 T. Shida and W. H. Hamill, *J. Phys. Chem.*, 1966, **44**, 4372; Y. Yamamoto, T. Aoyama and K. Hayashi, *J. Chem. Soc., Faraday Trans. I*, 1988, **84**, 2209.
- 48 X. Liu, K.-K. Iu, J. K. Thomas, H. He and J. Klinowski, *J. Am. Chem. Soc.*, 1994, **116**, 11 811.
- 49 K. Iu and J. K. Thomas, *J. Phys. Chem.*, 1991, **95**, 506.
- 50 I. K. Lednev, N. Mathivanan and L. J. Johnston, *J. Phys. Chem.*, 1994, **98**, 11.
- 51 F. Gessner and J. C. Scaiano, *J. Photochem. Photobiol. A: Chem.*, 1992, **67**, 91.
- 52 L. Brancalion, D. Brousmiche, V. J. Rao, L. J. Johnston and V. Ramamurthy, *J. Am. Chem. Soc.*, 1998, **120**, 4926.
- 53 F. L. Cozens, R. Bogdanova, M. Regimbald, H. Garcia, V. Marti and J. C. Scaiano, *J. Phys. Chem. B*, 1997, **101**, 6921.
- 54 P. D. Wood and L. J. Johnston, unpublished results.
- 55 P. Lakshminarasimahn and V. Ramamurthy, unpublished results; work in progress.
- 56 H. Frei, F. Blatter and H. Sun, *CHEMTECH.*, 1996, **26**, 24.

Paper 8/03871F